CHEMICAL ENGINEERING TRANSACTIONS
VOL. 57, 2017
A publication of AIDIC
The Italian Association of Chemical Engineering
Online at www.aidic.it/cet
Guest Editors: Sauro Pierucci, Jiří Jaromír Klemeš, Laura Piazza, Serafim Bakalis

ISBN978-88-95608- 48-8; **ISSN** 2283-9216

Mathematical Model of Pressure Crystallizer for High-Temperature Crystallization of Inorganic Compounds

Slawomir Misztal

Wroclaw University of Science and Technology, Faculty of Mechanical and Power Engineering, Wybrzeze Wyspianskiego 27, 50-370 Wroclaw, Poland
slawomir.misztal@pwr.edu.pl

A mathematical model of a pressure crystallizer for high-temperature crystallization of inorganic compounds from aqueous solutions is presented. The model is a result of long-term research which has led to the design of the new type continuous pressure crystallizer for high-temperature crystallization. High-temperature crystallization from aqueous solutions, also called crystallization under elevated temperature and pressure or thermal crystallization, can be used for salts characterized by inverse solubility (the solubility of some salts, mainly sulphates, decreases as the temperature rises). In order to crystallize such salts their solutions are heated up to appropriately high temperatures (in the order of 473 K). For this reasons the process of high-temperature crystallization takes place under elevated pressure (about 1.6 MPa). One of the main advantages of this process is lower energy consumption in comparison with evaporation crystallization, especially in the case of low-concentration solutions. The mathematical model is based on the results of investigations into the high-temperature crystallization of magnesium, manganese (II) and zinc sulphates conducted in the developed continuous pressure crystallizer with a working volume of 0.006 m^3. The crystallizer working space is divided into two parts. The upper part works similarly to the MSMPR crystallizer. From the crystallizer's upper part the crystal slurry flows to its lower part where the process is continued and where the crystal slurry thickens as some of the mother liquor with fines is discharged. Population balances for the crystallizer's upper part and its lower part, and kinetics parameters are entered into the mathematical model. Using the mathematical model one can simulate the effect of the operating parameters on the size of the produced crystals and generate designs of the pressure crystallizer.

1. Introduction

The aim of this work was to develop a mathematical model of a special continuous crystallizer for high-temperature crystallization, which could be used in its design. The model is a result of long-term research on this process (Misztal, 2002), which is also called crystallization under elevated temperature and pressure (Derry, 1972) or thermal crystallization (Fuller, 1966). The fact that the solubility of some salts (mainly sulphates) decreases as the temperature rises is exploited in the high-temperature crystallization process. In order to crystallize such salts their solutions are heated up to appropriately high temperatures (in the order of 473 K). For this reason the process of high-temperature crystallization takes place under elevated pressure (about 1.6 MPa). The main advantages of high-temperature crystallization are: a) lower energy consumption in comparison with evaporation crystallization, especially for low-concentration solutions (studies conducted in the USA show that in the case of manganese sulphate (II), the high-temperature crystallization energy demand is about 3-4 times lower in comparison with submerged combustion evaporation (Fuller, 1966)) and b) the salts are obtained in the form of monohydrates which are cheaper to transport and, because of their application, are often more sought after.

2. Experimental pressure crystallizer

A diagram of the specially developed experimental pressure crystallizer for high-temperature crystallization with a working volume of 0.006 m^3 is shown in Figure 1. The experimental set-up and the experimental

procedure were described in an earlier paper (Misztal, 2002). In the diagram $\dot{V}_i$, $\dot{V}$, $\dot{V}_F$, $\dot{V}_P$ denote the volumetric flow rates of respectively the inlet stream, the stream flowing from the crystallizer's upper part to its lower part, the fines stream and the product stream while n, n_F, n_P ,n_B stand for the population densities of crystals in respectively the crystallizer upper part, the fines, the product and the crystallizer bottom part.

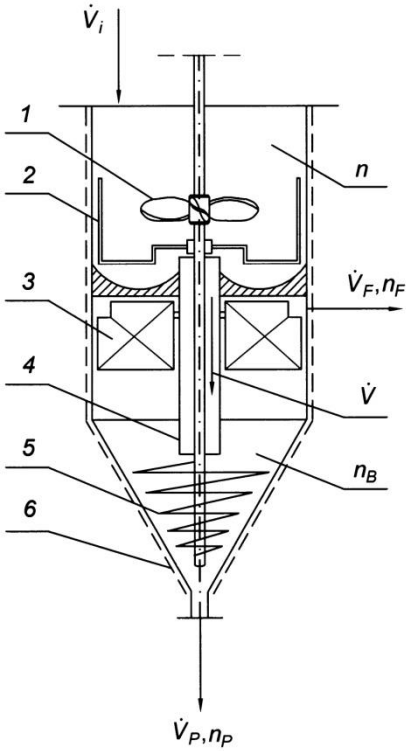

Figure 1: Pressure crystallizer diagram showing individual streams and population densities; 1- three-bladed propeller, 2 – anchor stirrer, 3 – baffles (six), 4 – overflow pipe, 5 – helical ribbon stirrer, 6 – electric heaters.

The crystallizer working space is divided into two parts. The upper part works similarly to the MSMPR crystallizer (Randolph, Larson, 1988). Near perfect mixing – one of the MSMPR crystallizer requirements – was confirmed by hydrodynamic investigations (Misztal, 2002). The thorough mixing of the crystal slurry in this zone is achieved owing to the use of propeller agitator (1) and a specially shaped bottom. In order to prevent incrustation on the apparatus wall specially designed anchor stirrer (2) was additionally installed. From the crystallizer upper part the crystal slurry flows through overflow pipe (4) to the crystallizer lower part where the process is continued at the expense of a further reduction in mother liquor supersaturation and where the crystal slurry thickens as some of the mother liquor with fines is discharged. A settling zone was created thanks to the use of six vertical baffles (3). Specially designed helical ribbon stirrer (5) stirs the crystal slurry in the lower part of the crystallizer. The stirrer ensures the thorough mixing of the slurry and prevents deposition of sediments on the wall of the conical bottom of the apparatus. The crystallizer is heated by electric heaters (6).

3. Mathematical model of crystallizer upper part. Kinetics of high-temperature crystallization

Assuming that the crystallizer's upper part is an MSMPR crystallizer and that the linear crystal growth rate is size independent, the population balance can be expressed as (Randolph and Larson, 1988):

$$G_T\left(\frac{dn}{dL}\right)+n=0 \tag{1}$$

When equation (1) is integrated, one gets:

$$n = n^0 \exp\left(-\frac{L}{G\tau}\right) \tag{2}$$

where: L – crystals size, G – linear crystal growth rate, τ - crystal slurry mean residence time, n^0 – nuclei population density. Using the semilogarithmic plot one can present relation (2) as a straight line and in this way determine G, n^0, and then calculate nucleation rate B from the relation:

$$B = n^0 G \tag{3}$$

The kinetic parameters of magnesium sulphate, manganese sulphate (II) and zinc sulphate were determined by taking samples of the crystal slurry from the crystallizer upper part (Misztal, 2002). An exemplary population density semilogarithmic plot is shown in Figure 2.

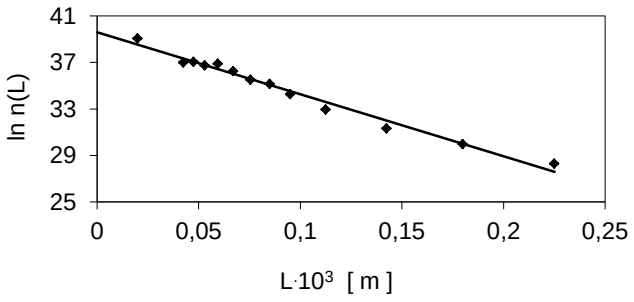

*Figure 2: Exemplary monohydrate magnesium sulphate crystals population density plot (*correlation coefficient R = 0.993).

Using the obtained data the secondary nucleation rate was estimated as (Beer and Mersmann, 1982):

$$B = kG^i M_t^j \varepsilon^h \tag{4}$$

where: ε – the specific power input, M_t – the concentration of crystals in the slurry, k – the nucleation rate coefficient and i, j, h – exponents (k, i, j, h were experimentally determined) (Misztal, 2002).

4. Mathematical model of crystallizer bottom part

Considering the design of the crystallizer described above, it was assumed that the perfect mixing of the slurry occurs in the crystallizer bottom part and that the removed product stream (without the volume of the settling zone from which the fines stream flows out) is unclassified. The population balance in the crystallizer bottom part can be expressed as:

$$V_2 \frac{d}{dL}\left[G_B(L) n_B\right] = \dot{V} n - \dot{V}_F n_F - \dot{V}_P n_P \tag{5}$$

where: V_2 – the crystallizer lower part volume without the volume of the settling zone in which, as assumed, no crystallization occurs (Randolph and Larson, 1988, Rojkowski and Synowiec, 1991), G_B – the linear crystal growth rate in the crystallizer lower part. By introducing the so-called withdrawal function (Randolph and Larson, 1988, Rojkowski and Synowiec, 1991) defined as:

$$C_w(L) = \frac{\dot{V}_F n_F + \dot{V}_P n_P}{\left(\dot{V}_F + \dot{V}_P\right) n_B} \tag{6}$$

one can write equation (5) as:

$$V_2 \frac{d}{dL}\left[G_B(L) n_B\right] = \dot{V} n - \left(\dot{V}_F + \dot{V}_P\right) C_w(L) n_B \tag{7}$$

The kinetics investigations confirmed that the linear crystal growth rate is size independent. Therefore it can be assumed that also the crystal growth rate in the crystallizer bottom part (G_B) does not depend on the size of the crystals. At $L < L_F$, where L_F is the fines cut size (the maximum fines size), it was assumed that population density n_F is approximately equal to the crystals population density in the crystallizer lower part,

i.e. $n_F(L) = n_B(L < L_F)$ (Rojkowski and Synowiec, 1991). Since the product stream is unclassified the product crystals size distribution corresponds to the crystals size distribution in volume V_2 of the lower part of the crystallizer, and so $n_B(L) = n_P(L)$. Assuming (Rojkowski and Synowiec, 1991) that:

$$\dot{V} = \dot{V}_F + \dot{V}_P \tag{8}$$

and the mean residence time of crystal slurry:

$$\tau_B = \frac{V_2}{\dot{V}} \tag{9}$$

and substituting the withdrawal function value, which for the above assumptions at $L < L_F$ amounts to:

$$C_w(L) = \frac{\left(\dot{V}_F + \dot{V}_P\right) n_P}{\left(\dot{V}_F + \dot{V}_P\right) n_B} = 1 \tag{10}$$

equation (7) becomes:

$$\frac{dn_B}{d_L} + \frac{n_B}{G_B \tau_B} = \frac{n}{G_B \tau_B} \tag{11}$$

Substituting

$$n = n^0 \exp\left(-\frac{L}{G\tau}\right) \tag{12}$$

for the population density in the crystallizer upper part, equation (11) can be written as:

$$\frac{dn_B}{dL} + \frac{n_B}{G_B \tau_B} = \frac{n^0 \exp\left(-\frac{L}{G\tau}\right)}{G_B \tau_B} \tag{13}$$

The solution of this equation at initial condition $n_B(0) = n_B^0$ has the form:

$$n_B(L < L_F) = n_B^0 \exp\left(-\frac{L}{G_B \tau_B}\right) + \frac{n^0 G\tau}{G\tau - G_B \tau_B}\left[\exp\left(-\frac{L}{G\tau}\right) - \exp\left(-\frac{L}{G_B \tau_B}\right)\right] \tag{14}$$

Using equation (14) and adopting the earlier assumption that $n_F(L) = n_B(L < L_F)$, one gets the following relation for the concentration of crystals in the slurry flowing out as fines stream $\dot{V}_F$ from the settling zone:

$$M_{tF} = f_V \rho_s \int_0^{L_F} n_F L^3 dL \tag{15}$$

where: f_V – a volumetric shape factor, ρ_s – crystal density.

After the integration of equation (15) and the substitution of the equations:

$$n^0 G = k G^i M_t^j \varepsilon^h \tag{16}$$

$$n_B^0 G_B = k G_B^i M_{tB}^j \varepsilon_B^h \tag{17}$$

where: M_{tB} – the concentration of crystals in the slurry in the bottom part of the crystallizer, ε_B – the specific power input in the bottom part of the crystallizer, n_B^0 – the nuclei population density in the bottom part of the crystallizer; equation (15) has the form:

$$M_{tF} = 6 f_V \rho_s k \left[G_B^i M_{tB}^j \varepsilon_B^h \tau_B \left(G_B \tau_B\right)^3 A + \frac{G^i M_t^j \varepsilon^h \tau (G\tau)^4}{G\tau - G_B \tau_B} B - \frac{G^i M_t^j \varepsilon^h \tau \left(G_B \tau_B\right)^4}{G\tau - G_B \tau_B} A\right] \tag{18}$$

where:

$$A = 1 - exp\left(-\frac{L_F}{G_B\tau_B}\right)\left[1 + \frac{L_F}{G_B\tau_B} + \frac{1}{2}\left(\frac{L_F}{G_B\tau_B}\right)^2 + \frac{1}{6}\left(\frac{L_F}{G_B\tau_B}\right)^3\right] \tag{19}$$

$$B = 1 - exp\left(-\frac{L_F}{G\tau}\right)\left[1 + \frac{L_F}{G\tau} + \frac{1}{2}\left(\frac{L_F}{G\tau}\right)^2 + \frac{1}{6}\left(\frac{L_F}{G\tau}\right)^3\right] \tag{20}$$

Since $n_F = 0$ at $L > L_F$ the withdrawal function value amounts to:

$$C_w(L) = \frac{\dot{V}_P n_P}{(\dot{V}_F + \dot{V}_P) n_B} = 1 - s \tag{21}$$

where:

$$s = \frac{\dot{V}_F}{\dot{V}_F + \dot{V}_P} \tag{22}$$

The population balance for this case is described by the equation:

$$V_2 \frac{d}{dL}[G_B(L) n_B] = \dot{V} n - (\dot{V}_F + \dot{V}_P)(1 - s) n_B \tag{23}$$

Taking into account equations (8), (9) and (12) and that the linear crystal growth rate is size independent one gets the equation:

$$\frac{dn_B}{dL} + \frac{(1-s)n_B}{G_B\tau_B} = \frac{n^0 exp\left(-\frac{L}{G\tau}\right)}{G_B\tau_B} \tag{24}$$

The initial condition for this equation is obtained using equation (14) in the form:

$$n_B(L_F) = n_B^0 exp\left(-\frac{L_F}{G_B\tau_B}\right) + \frac{n^0 G\tau}{G\tau - G_B\tau_B}\left[exp\left(-\frac{L_F}{G\tau}\right) - exp\left(-\frac{L_F}{G_B\tau_B}\right)\right] \tag{25}$$

On this basis one gets the solution of equation (24):

$$\begin{aligned} n_B(L > L_F) &= n_B^0 exp\left[-\frac{sL_F}{G_B\tau_B} + \frac{(s-1)L}{G_B\tau_B}\right] + \\ &+ \frac{n^0 G\tau}{(1-s)G\tau - G_B\tau_B}\left[exp\left(-\frac{L}{G\tau}\right) - exp\left(-\frac{L_F}{G\tau} - \frac{(s-1)L_F}{G_B\tau_B} + \frac{(s-1)L}{G_B\tau_B}\right)\right] + \\ &+ \frac{n^0 G\tau}{G\tau - G_B\tau_B}\left[exp\left(-\frac{L_F}{G\tau} - \frac{(s-1)L_F}{G_B\tau_B} + \frac{(s-1)L}{G_B\tau_B}\right) - exp\left(-\frac{sL_F}{G_B\tau_B} + \frac{(s-1)}{G_B\tau_B}\right)\right] \end{aligned} \tag{26}$$

The experimental studies showed that the fraction of crystals of size less than L_F in the product is very small by mass (on average amounting to about 1% for the three tested salts) and practically has no effect on the mass size distribution of the obtained crystals. Therefore the applicability of equation (26) can be extended to cover the range $0 < L < L_F$ whereby one can obtain the following relation for the concentration of crystals in the slurry in the bottom part of the crystallizer:

$$M_{tB} = f_V \rho_s \int_0^\infty n_B L^3 dL \tag{27}$$

Similarly, the concentration of crystals in the slurry in the crystallizer bottom part for the size range of 0–L can be expressed by the equation:

$$M = f_V \rho_s \int_0^L n_B L^3 dL \tag{28}$$

Having equations (27) and (28) and taking into account the fact that the concentration of crystals in the slurry (the product) leaving the crystallizer is equal to the concentration of crystals in the slurry in the crystallizer bottom part (M_{tB}) one gets the following relation for the cumulative mass size distributions of crystals in the product:

$$Q(L) = \frac{M}{M_{tB}} \tag{29}$$

Owing to the experimental studies of the crystallizer, consisting in determining the kinetic parameters of the high-temperature crystallization and the effect of: a) mean crystal slurry residence time, b) crystal slurry density and c) specific power input (in the upper and bottom part of the crystallizer) on the size distribution of the obtained crystals of monohydrate magnesium sulphate, monohydrate manganese sulphate (II) and monohydrate zinc sulphate (Misztal, 2002), it was possible to compare the experimental cumulative mass size distributions of crystals (*Q(L)* obtained in the individual trials with the distributions calculated from equation (29) and thus to verify the model. Figure 3 shows exemplary calculated and experimental cumulative mass size distributions of monohydrate magnesium sulphate crystals produced in the pressure crystallizer.

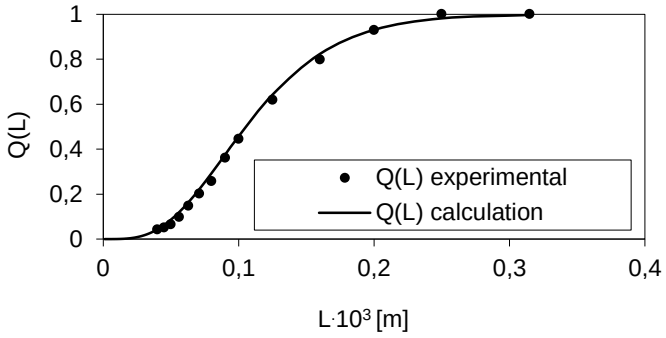

Figure 3: Exemplary calculated and experimental cumulative mass size distributions of monohydrate magnesium sulphate crystals produced in pressure crystallizer (R = 0.998).

5. Conclusions

The crystal size distributions calculated using the mathematical model are in good agreement with the experimental ones. This shows that the assumptions made are correct and that the population balance can be used to create such a model and to determine the kinetic parameters of high-temperature crystallization. Using the mathematical model one can develop a method of generating designs of the new continuous pressure crystallizer for high-temperature crystallization, which increases the chances of its application in industry. This would result in great energy savings, especially in the case of the crystallization of inorganic compounds from low-concentration solutions since the expensive concentration of the latter would no longer be necessary. The proposed mathematical model can also be used to select pressure crystallizer operating parameters to obtain proper sizes of crystals, ensuring a high rate of their filtration and drying.

Reference

Beer W.F., Mersmann A.B., 1982, The influence of power input and suspension density on the crystallization kinetics of KCL in a continuous draft tube crystallizer, Industrial Crystallization 81. Proceedings of the 8th Symposium on Industrial Crystallization, Budapest, Hungary, 28-30 September, 1981, Eds. Jancic S.J., de Jong E.J., North-Holland, Amsterdam, the Netherlands, 209-215.

Derry R., 1972, Pressure Hydrometallurgy: A Review, Minerals Sci. Eng. 4, 1, 3-24.

Fuller H.C., 1966, Recovery of manganese sulphate crystals from solution by submerged combustion evaporation and thermal crystallization, Rep. Invest. 6762, U.S. Dept. of the Interior, Bureau of Mines, Washington, USA, 1-30.

Misztal S., 2002, High-temperature crystallization of inorganic compounds from aqueous solutions, Chemical Engineering Transactions, Volume 1, Proceedings of 15th International Symposium on Industrial Crystallization, Sorrento, Italy, 1077-1082.

Randolph A.D., Larson M.A., 1988, Theory of particulate processes, Academic Press Inc., San Diego, USA.

Rojkowski Z., Synowiec J., 1991, Crystallization and crystallizers, WNT, Warsaw, Poland (in Polish).